J|A|C|S
ARTICLES
Published on Web 03/12/2002

Photogeneration and Quenching of Reactive Oxygen Species by Urocanic Acid

Nicole Haralampus-Grynaviski,[†] Carla Ransom,[†] Tong Ye,[†]
Małgorzata Rôżanowska,[§] Marta Wrona,[§] Tadeusz Sarna,[§] and John D. Simon*[,†,‡]

Contribution from the Department of Chemistry, Duke University, Durham, North Carolina 27708, Department of Biochemistry, Duke University Medical Center, Durham, North Carolina 27710, and Institute of Molecular Biology, Jagiellonian University, Al Mickiewicza 3, PL 31120 Krakow, Poland

Received August 21, 2001

Abstract: Urocanic acid, UCA, is characterized by two electronic transitions in the UV-B (280−320 nm) which comprise its broad absorption spectrum and give rise to wavelength-dependent isomerization quantum yields. The absorption spectrum of UCA extends into the UV-A (320−400 nm). Given the UV-A component of sunlight is significantly greater than the UV-B component it is hypothesized even weak UV-A photochemistry of UCA could be important for in vivo responses to UV radiation. Degenerate pump−probe experiments performed on *t*-UCA at several wavelengths in the UV-A reveal an excited-state absorption that undergoes a rapid, ∼1 ps decay. Photoacoustic experiments performed on both the cis and trans isomers reveal the formation of a long-lived intermediate following UV-A excitation. The efficiency and action spectra for this latter photoactive process are presented and are similar for both isomers of UCA. Cholesterol hydroperoxide assays designed to investigate the nature of the UV-A photoreactivity of *t*-UCA confirm the production of reactive oxygen species. The bimolecular rate constant for the quenching of singlet oxygen by *t*-UCA is determined to be 3.5×10^6 M^{-1} s^{-1}. Taking into consideration recent theoretical calculations and jet expansion studies of the electronic structure of gas-phase *t*-UCA, a model is proposed to explain the isomerization and photoreactivity of *t*-UCA in solution over the UV-A region.

Introduction

Urocanic acid (UCA) is one of the primary UV absorbing chromophores in the stratum corneum of human skin. UCA is formed initially as the trans isomer, *t*-UCA. Upon absorption of light, the naturally occurring *t*-UCA isomerizes to the cis form, *c*-UCA. Under solar illumination, the in vitro photostationary state is approximately 30% *t*-UCA and 70% *c*-UCA.[1,2] Because the enzyme urocanase is not present in skin, UCA accumulates until it is removed through sweat or during the monthly skin renewal process.[3] Reported concentrations of UCA in skin vary widely. An estimation of UCA concentration within the human epidermis of 0.3 to 8.9 mM by Laihia et al. was derived from analyzing several published studies.[4]

Due to its strong absorption in the UV, UCA was initially viewed as a natural sunscreen. In the early 1980s, however, it was discovered the UCA absorption spectrum matches the action spectra for immune suppression of contact hypersensitivity.[5,6] Since then there has been considerable research on UCA, particularly *c*-UCA, as a mediator for UV-induced immune suppression. Researchers find there is evidence that *c*-UCA suppresses contact hypersensitivity that and delayed hypersensitivity reduces the Langerhans cell count in the epidermis, prolongs skin-graft survival time, and affects natural killer cell activity.[7−9] There are currently several proposed models for how *c*-UCA causes these biologic effects including the following: regulation of cyclic AMP synthesis,[10] mast cell degranulation,[11,12] and cytokine level modulation.[13−15] After 20 years of research, a *c*-UCA receptor in skin that could explain its physiochemical action has not been identified.[16] Recently oxidative products of UCA are proposed to be responsible for some of the UV-induced immune suppression.[17−19] Because such products can be gener-

* Corresponding author. E-mail: jds@chem.duke.edu.
[†] Duke University.
[§] Jagiellonian University.
[‡] Duke University Medical Center.

(1) Morrison, H.; Avnir, D.; Bernasconi, C.; Fagan, G. *Photochem. Photobiol.* **1980**, *32*, 711−714.
(2) Morrison, H.; Avnir, D.; Zarrella, T. *J. Chromatogr.* **1980**, *183*, 83−86.
(3) Baden, H. P.; Pathak, M. A. *J. Invest. Dermatol.* **1967**, *48*, 11−17.
(4) Laihia, J. K.; Attila, M.; Neuvonen, K.; Pasanen, P.; Tuomisto, L.; Jansen, C. T. *J. Invest. Dermatol.* **1998**, *111*, 705−706.
(5) De Fabo, E.; Noonan, F.; Fisher, M.; Burns, J.; Kacser, H. *J. Invest. Dermatol.* **1983**, *80*, 319−319.
(6) Noonan, F. P.; De Fabo, E. C. *Immunol. Today* **1992**, *13*, 250−254.
(7) Bi, Z. G.; Wang, T.; Chen, H. Q.; Ni, L.; Ding, X. J. *Chin. Med. J.* **1998**, *111*, 372−372.
(8) Kondo, S.; Sauder, D. N.; McKenzie, R. C.; Fujisawa, H.; Shivji, G. M.; ElGhorr, A.; Norval, M. *Immunol. Lett.* **1995**, *48*, 181−186.
(9) Reeve, V. E.; Ley, R. D.; Reilly, W. G.; Bosnic, M. *Int. Arch. Allergy Immunol.* **1996**, *109*, 266−271.
(10) Bouscarel, B.; Noonan, F.; Ceryak, S.; Gettys, T. W.; Phillips, T. M.; De Fabo, E. C. *Photochem. Photobiol.* **1998**, *67*, 324−331.
(11) Hart, P. H.; Grimbaldeston, M. A.; Swift, G. J.; Hosszu, E. K.; Finlay-Jones, J. J. *Photochem. Photobiol.* **1999**, *70*, 807−812.
(12) Wille, J. J.; Kydonieus, A. F.; Murphy, G. F. *Skin Pharmacol. Appl. Skin Physiol.* **1999**, *12*, 18−27.
(13) Redondo, P.; GarciaFoncillas, J.; Cuevillas, F.; Espana, A.; Quintanilla, E. *Photodermatol. Photoimmunol. Photomed.* **1996**, *12*, 237−243.
(14) Shen, J.; Bao, S.; Reeve, V. E. *J. Invest. Dermatol.* **1999**, *113*, 1059−1064.
(15) Reeve, V. E.; Bosnic, M.; Nishimura, N. *J. Invest. Dermatol.* **1999**, *112*, 945−950.

Scheme 1. The Molecular Structures for Neutral *t*-UCA and *c*-UCA

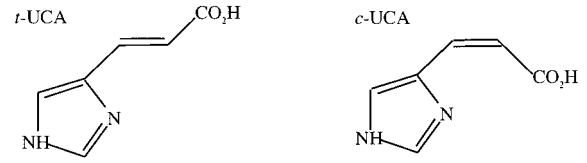

ated photochemically, it is important to understand the UV-A-induced photoreaction of UCA and whether the reactivity differs between the two isomers.

Scheme 1 shows the structure of the two isomers of UCA. There are three protonation sites on the molecule. The pK_a values for *t*-UCA are 3.5 for the carboxylic acid moiety, 5.8 for the tertiary nitrogen, and 13 for the secondary nitrogen.[20,21] Under physiological conditions, UCA exists as either a zwitterion (pH sweat ~5.6) or an anion (pH living cell ~7). The absorption spectra for the two isomers are identical in shape but differ in intensity. The absorption coefficient of *c*-UCA, at its absorption maximum, is 70% of that of *t*-UCA.[16] The absorption spectrum of UCA depends on pH.[21] In pH 5.6 and 7.3 solutions, the absorption spectrum of *t*-UCA peaks at 270 and 280 nm, respectively.

Previous work shows that while the anionic form of *t*-UCA (pH 7.2) has a red-shifted absorption relative to the zwitterionic form (pH 5.6), the two forms emit from a common excited state.[22] Specifically, for *t*-UCA excited at 264 nm (pH 3.2−11.0), there is weak fluorescence with an emission peak around 365 nm, independent of pH. The fluorescence excitation spectrum shows a peak around 280 nm, also independent of pH.[22] Ultrafast pump−probe experiments exciting *t*-UCA at 266 nm in pH 5.5 and 7.2 solutions show similar transients.[23] These collective results support the conclusion UV-B excitation near the peak absorption results in the rapid deprotantion of *t*-UCA at pH 5.6, thereby generating a molecule with a similar electronic structure to the anionic form of *t*-UCA present in a solution of pH 7.2.

The isomerization quantum yield for *t*-UCA is wavelength dependent. The isomerization efficiency peaks at 313 nm (on the red edge of the absorption spectrum) with a quantum yield, Φ, of 0.49, and is reduced near the absorption maximum (at 264 nm) with a Φ of 0.05.[24] Most previous photochemical studies on *t*-UCA focused on understanding this wavelength-dependent isomerization. Excitation near the peak of *t*-UCA absorption at 266 nm results in excitation to an excited singlet state from which there results rapid and efficient intersystem crossing to the triplet manifold and negligible isomerization. The triplet state persists onto at least the 10 ns time scale in deoxygenated solvents.[23] Excitation of *t*-UCA absorption at 310 nm results in excitation to a different excited singlet state from which there is significant isomerization and no evidence of formation of a long-lived triplet.[25] Femtosecond time-resolved absorption and photoacoustic experiments established the wavelength-dependent isomerization quantum yields arise from the excitation of these two overlapping electronic transitions in the UV-B underlying the broad featureless absorption spectrum of *t*-UCA.[26]

Recently de Fabo and co-workers reported evidence of *t*-UCA isomerization occurring throughout the UV-A region.[27] In addition, previous photochemical studies of Morrison and co-workers indicate radical production following the UV-A photoexcitation of *t*-UCA.[19] While the absorption cross section of *t*-UCA in the UV-A is quite small, these data suggest the molecule exhibits a rich photochemistry in this region. In this paper we use a variety of spectroscopic techniques to examine the photochemical behavior of UCA in the UV-A. In addition, building upon newly published supersonic jet experiments on *t*-UCA by Ryan and Levy[28] and theoretical calculations by Page et al,[29] a model for the electronic structure of *t*-UCA accounting for the range of photochemical behavior observed in the UV-B and UV-A is proposed.

Experimental Section

Samples. *t*-UCA was purchased from Aldrich and is used without further purification. To generate *c*-UCA, a saturated aqueous solution of *t*-UCA is irradiated with sunlight or a UV lamp (Mineralight lamp, Model UVGL-25) to generate a mixture of the two isomers. The *c*-UCA isomer is isolated from this solution as previously described.[25,30] All solutions are prepared in phosphate buffer for experiments.

Steady-State Absorption. Absorption spectra are recorded with a Hewlard Packard UV−vis spectrophotometer model 8452A with a 1 cm quartz cuvette. Fluorescence spectra of *t*-UCA are measured on a Perkin-Elmer LS-50B fluorometer.

Femtosecond Transient Absorption. Femtosecond time-resolved spectroscopy is performed with an experimental setup previously described.[31] A Spectra Physics laser system consisting of a titanium-sapphire regenerative amplifier (Spitfire) and an OPA (model 800) is used to generate tunable UV-A pulses approximately 300 fs in duration. The pulse energies are controlled with neutral density filters, and for the experiments reported, the pump and probe pulses are on the order of 100 and 10 nJ, respectively. The polarization of the pump and probe pulses is set to magic angle.

For degenerate pump−probe experiments at 310, 320, and 330 nm, the concentration of *t*-UCA in a pH 7.3 solution is set to give an absorbance of ~0.20 in a 1 mm cuvette at the excitation wavelength. Sample solutions are run through a 1 mm flow cell and the absorptions of the solutions do not change by more than 0.01 absorbance units over the course of an experiment. An identical procedure is used for studies conducted at pH 5.6.

Pulsed-Laser Photoacoustic Spectroscopy. Photoacoustic experiments are done with a similar experimental design and method of analysis as previously described.[32] The same tunable laser system

(16) Mohammad, T.; Morrison, H.; HogenEsch, H. *Photochem. Photobiol.* **1999**, *69*, 115−135.
(17) Kammeyer, A.; Eggelte, T. A.; Overmars, H.; Bootsma, A.; Bos, J. D.; Teunissen, M. B. M. *Biochim. Biophys. Acta-Gen. Subj*. **2001**, *1526*, 277−285.
(18) Ramu, A.; Mehta, M. M.; Leaseburg, T.; Aleksic, A. *Cancer Chemother. Pharmacol.* **2001**, *47*, 338−346.
(19) Morrison, H.; Deibel, R. M. *Photochem. Photobiol.* **1988**, *48*, 153−156.
(20) Roberts, J. D.; Yu, C.; Flanagan, C.; Birdseye, T. R. *J. Am. Chem. Soc.* **1981**, *104*, 3945−3949.
(21) Mehler, A. H.; Tabor, H. *J. Biol. Chem.* **1953**, *201*, 775−784.
(22) Shukla, M. K.; Mishra, P. C. *Spectrochim. Acta, Part A* **1995**, *51*, 831−838.
(23) Li, B.; Hanson, K. M.; Simon, J. D. *J. Phys. Chem. A* **1997**, *101*, 969−972.
(24) Morrison, H.; Bernasconi, C.; Pandey, G. *Photochem. Photobiol.* **1984**, *40*, 549−550.
(25) Hanson, K. M.; Li, B.; Simon, J. D. *J. Am. Chem. Soc.* **1997**, *119*, 2715−2721.
(26) Hanson, K. M.; Simon, J. D. *Photochem. Photobiol.* **1998**, *67*, 538−540.
(27) Webber, L. J.; Whang, E.; De Fabo, E. C. *Photochem. Photobiol.* **1997**, *66*, 484−492.
(28) Ryan, W. L.; Levy, D. H. *J. Am. Chem. Soc.* **2001**, *123*, 961−966.
(29) Page, C. S.; Olivucci, M.; Merchan, M. *J. Phys. Chem. A* **2000**, *104*, 8796−8805.
(30) Anglin, J. H.; Everett, M. A. *Biochim. Biosphys. Acta* **1964**, *88*, 492−501.
(31) Floyd, J. S.; Haralampus-Grynaviski, N.; Ye, T.; Zheng, B.; Simon, J. D.; Edington, M. D. *J. Phys. Chem. B* **2001**, *105*, 1478−1483.
(32) Nofsinger, J. B.; Forest, S. E.; Simon, J. D. *J. Phys. Chem. B* **1999**, *103*, 11428−11432.

mentioned above is used with the excitation pulses set to ~5 μJ in energy. The reference compound bromocresol purple, BCP, releases 100% of its absorbed energy promptly as heat to the solvent.[33] For both UCA and BCP, it was confirmed contributions to the acoustic wave from volume changes are negligible.[25] The sample concentrations are adjusted so the absorption is ~0.10 in a 1 cm cuvette at each wavelength studied. For each set of runs, the UCA and reference BCP absorption are matched exactly. The absorption of the solutions did not change by more than 0.01 over the course of an experiment. Because of the low extinction coefficient for UCA in a pH 7.3 solution, photoacoustic measurements were not possible for wavelengths longer than 350 nm. Solutions are bubbled with argon or oxygen for 10 min prior to each experiment.

Quenching of Singlet Oxygen. The rate constant for the quenching of singlet oxygen, $^1O_2$, by *t*-UCA is determined by quantifying the $^3\Sigma \leftarrow {}^1\Delta_g$ emission (1270 nm) from oxygen following excitation of rose bengal, RB, in the presence of *t*-UCA in a D_2O solution. RB is photoexcited at 532 nm with the second harmonic of a Nd:YAG laser. The RB absorbance is 0.1 in a 1 cm cuvette at 532 nm for all the solutions. The concentration of *t*-UCA is varied from 0 to 12 mM.

Cholesterol Hydroperoxide Assay. Photoinduced radical chemistry and singlet oxygen chemistry of *t*-UCA are studied with use of a cholesterol hydroperoxide assay as previously described.[34] Specifically, liposomes made of dimyristoyl phosphatidylcholine, DMPC, and cholesterol (2 mM each) are mixed and suspended in buffered H_2O (or D_2O) with and without 5 mM *t*-UCA. Higher concentrations of *t*-UCA (10 mM) and cholesterol (4 mM) are also run. These samples are irradiated under air with 310−400 nm light (21.8 mW/cm^2) and aliquots are extracted as a function of irradiation time. HPLC analysis is used to separate and quantify the photochemically generated cholesterol hydroperoxides 5α-ChOOH and 7α/β-ChOOH (5α-ChOOH = 3β-hydroxy-5α-cholest-6-ene-5-hydroperoxide, 7α/β-ChOOH = 3β-hydroxycholest-5-ene-7α-hydroperoxide and 3β-hydroxycholest-5-ene-7β-hydroperoxide.) The optimal detection limit for these products is generally on the order of ~1 pmol.[35,36] Due to background signals which could not be eliminated, the detection limit for the experiments with *t*-UCA was on the order of ~0.3 nmol. Similar experiments are also performed without liposomes present in a homogeneous 2-propanol solvent with 3 mM *t*-UCA. Each set of experiments was repeated at least three times on independently prepared smaples.

Results

Steady-State Absorption. Buffered 0.1 mM *t*-UCA solutions were made at pH 3.0, 5.6, 7.3, and 13. These pH values were chosen so the dominant species in solution are the cation, zwitterion, anion, and dianion, respectively.[16] Figure 1 shows the resulting absorption spectra. To study the photophysical properties of *t*-UCA in the UV-A at physiological pH requires using high (near saturation) concentrations. It is important to verify under these conditions that the absorption does not arise from the aggregation of molecules. To check this, pH 7.3 solutions containing concentrations of *t*-UCA ranging from 10 to 0.01 mM were prepared and the absorption spectra recorded. Figure 2 shows the log of the *t*-UCA absorption values at different wavelengths plotted along the log of the *t*-UCA concentration along with least-squares linear fits. The slope from the linear fits is ~1.0 for all wavelengths from 277 to 340 nm, confirming the absorption depends linearly on concentration. In

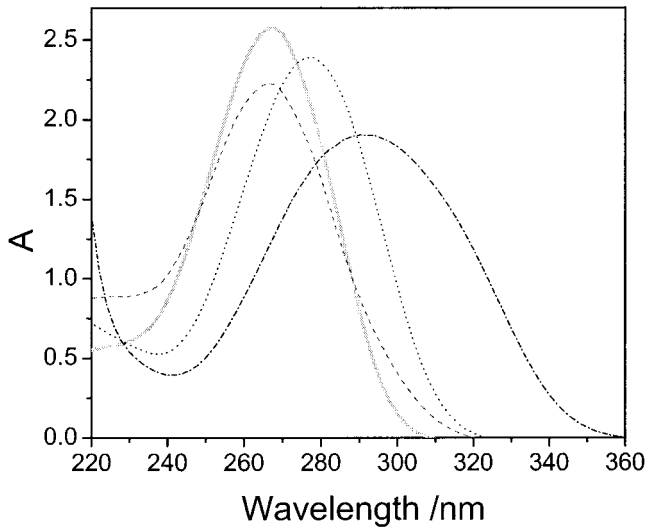

Figure 1. The absorption spectra for 0.1 mM *t*-UCA at pH 3.0 (solid), 5.6 (dash), 7.3 (dot), and 13 (dash−dot) are shown. Note that comparing pH 5.6 to 7.3 (biologically relevant values of pH) the absorption maximum of *t*-UCA shifts from 270 to 280 nm.

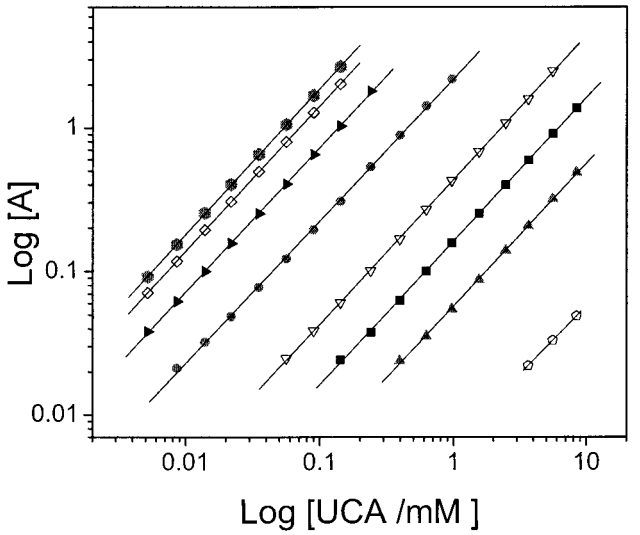

Figure 2. For *t*-UCA at pH 7.3, the log of the absorption at several wavelengths is shown plotted against the log of the concentration of *t*-UCA. A linear regression fit for each wavelength ($r^2 \sim 0.99$) is shown. The slope is 1.0 for all lines. From left to right the wavelengths are 280, 290, 300, 310, 320, 325, 330, and 340 nm.

agreement with previously reported experiments,[22,37] the quantum yield for *t*-UCA fluorescence is found to be very weak, around 10^{-4}.

Femtosecond Transient Absorption. Figure 3 shows transient absorption kinetics following UV-A excitation of *t*-UCA in a pH 7.3 solution. The femtosecond degenerate pump−probe data show no wavelength dependence over the range examined (310−330 nm). Immediately following excitation a transient absorption is observed, which rapidly decays. No evidence of a long-lived state or residual bleach of the ground state is observed. A single-exponential fit to these data indicates the transient decays with a 0.95 ± 0.5 ps time constant. We had previously reported degenerate experiments at 306 nm which exhibited a transient bleach that recovered with a time constant of ~100 ps.[23] This previous data is found to be an artifact

(33) Braslavsky, S. E.; Heibel, G. E. *Chem. Rev.* **1992**, *92*, 1381−1410.
(34) Rozanowska, M.; Jarvis-Evans, J.; Korytowski, W.; Boulton, M. E.; Burke, J. M.; Sarna, T. *J. Biol. Chem.* **1995**, *270*, 18825−18830.
(35) Korytowski, W.; Bachowski, G. J.; Girotti, A. W. *Anal. Biochem.* **1991**, *197*, 149−156.
(36) Korytowski, W.; Bachowski, G. J.; Girotti, A. W. *Anal. Biochem.* **1993**, *213*, 111−119.
(37) Hanson, K. M.; Simon, J. D. *Abstr. Pap. Am. Chem. Soc.* **1997**, *213*, 396-PHYS.

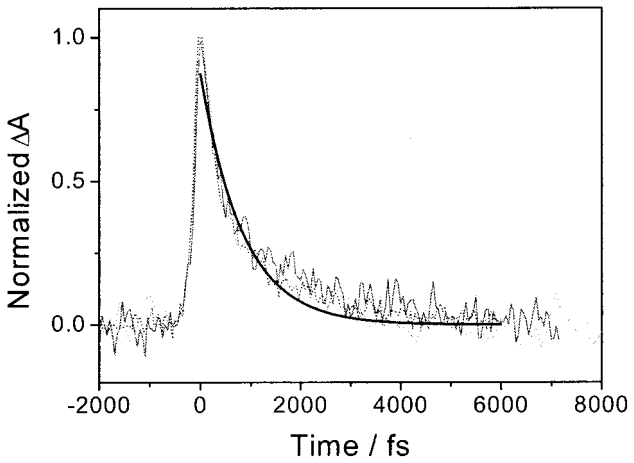

Figure 3. The degenerate 310 (solid), 320 (dash), and 330 nm (dot) pump probe transients for *t*-UCA at pH 7.3 are shown. The single-exponential decay fit (black line) shown gives a lifetime for the transient species of 0.950 ps ($r^2 \sim 0.93$).

Table 1. Percent Heat Released, ϕ, by *c*-UCA and *t*-UCA in Argon Saturated Solutions as a Function of UV-A Excitation Wavelength (error ±5%)

ϕ	*c*-UCA(Ar)	*t*-UCA(Ar)
310 nm	97	89
320 nm	73	52
330 nm	67	45
350 nm	57	47

attributed to the high-energy excitation pulses used in the earlier experiment. The time constant reported herein indicates a more rapid repopulation of the ground state and therefore does not change any of the conclusions reached in the previous paper.[23]

A degenerate 310 nm experiment on *t*-UCA in a pH 5.6 solution shows similar, but not identical, kinetics to that observed at pH 7.3. At pH 5.6, the decay is biphasic exhibiting a <0.2 ps component (data not shown). Previously experiments establish excitation at this pH results in rapid deprotonation of UCA,[23] and so this ultrafast component is assigned to the deprotonation process.

Pulsed-Laser Photoacoustic Spectroscopy. Figure 4 shows the photoacoustic signal for *t*-UCA and BCP at 310 and 320 nm in oxygen and argon saturated solutions. The 310 nm data show the reference BCP and *t*-UCA signal curves being nearly equivalent in amplitude meaning *t*-UCA releases nearly all of its absorbed energy. The 320 nm data show *t*-UCA retains significant energy, hence the lower signal amplitude relative to the reference BCP signal. The absence of any time delays between the *t*-UCA and BCP photoacoustic waves indicates the kinetics of formation and lifetime of the intermediate are outside the temporal response of the instruments (<1 and >100 ns, respectively).[38]

The fraction of the absorbed energy released as heat (ϕ) following excitation of UCA can be quantified from the photoacoustic data by taking the ratio of the amplitudes of the UCA and BCP signals normalized by their absorption values. This percent heat release can be equated with an absolution energy released (Q) using $Q = \phi E_{h\nu}$, where $E_{h\nu}$ is the energy of the excitation pulse. Table 1 lists the value of ϕ for *c*-UCA and *t*-UCA in argon saturated solutions at different UV-A wavelengths. As exemplified by the data in Figure 4, the value of ϕ for aerobic samples typically showed an increase of 5% to 10% compared to the anaerobic samples for both isomers.

Quenching of Singlet Oxygen. In Figure 5 the reciprocal of the measured $^1O_2$ lifetime, $1/\tau$, as a function of the *t*-UCA concentration is shown. The data are fit to the Stern−Volmer equation: $1/\tau = 1/\tau^0 + k_q$ [*t*-UCA], where the intercept should give the lifetime of $^1O_2$ in the absence of *t*-UCA and the slope gives the bimolecular rate constant for quenching. A straight line is observed indicating there is no quenching of the sensitizer RB by *t*-UCA. From data in the Figure 5, the intercept gives 1.56×10^4 s^{-1} for $1/\tau^0$, which is in excellent agreement with literature values for this lifetime.[39] From the slope, the bimolecular rate constant for $^1O_2$ quenching by *t*-UCA, k_q, is determined to be 3.5×10^6 M^{-1} s^{-1}.

Cholesterol Hydroperoxide Assay. The cholesterol hydroperoxide assay is a sensitive method for determining the photogeneration of reactive oxygen species. In addition, the formation of the 5α-ChOOH product is a unique marker for the presence of $^1O_2$. The 7α/β-ChOOH products, on the other hand, generally reflect secondary reactions or free radical derived attack.[35,40] HPLC traces showing the presence of 7α/β-ChOOH and 5α-ChOOH generated from the UV-A excitation of *t*-UCA are shown in Figure 6 for the 2-propanol solvent. These data clearly show that the hydroperoxides are formed and that the signals are significant in comparison to the background.

In the presence of *t*-UCA, there is enhanced formation of 7α/β-ChOOH compared to the control experiment in the absence of *t*-UCA whether the experiments are done in liposomes or 2-propanol (Figure 7). Furthermore, as can be decuced from the difference in the concentration units on the *y*-axis, the rate of production of 7α,β-ChOOH is a factor of 2 greater in D_2O relative to H_2O.

For the 2-propanol solution, the formation of 5α-ChOOH in the presence of *t*-UCA is increased relative to the control. However, for the liposome experiments UV-A irradiation of the cholesterol control with no *t*-UCA results in ~10% greater production of 5α-ChOOH. than in the presence of *t*-UCA (Figure 7,A,B). Despite all attempts to purify the components used to generate the liposomal solutions containing cholesterol and DMPC, this background signal could not be eliminated. It was, however, reproducible. The rate of production of 5α-ChOOH in D_2O is 2 times greater than that of H_2O for both *t*-UCA and control solutions.

Discussion

Before discussing the UV-A-induced photoreactivity of UCA, it is necessary to consider the possible effects associated with the large range in concentrations used in the different experimental studies performed. Previous experiments reported concentration-dependent excitation spectra of *t*-UCA; with increasing concentration, the spectrum red shifts.[22] This was attributed to changes in the relative populations of several ground-state rotamers of *t*-UCA. Photochemical dimerization of *t*-UCA has also been reported, suggesting that association between UCA molecules can occur.[41] In the course of the studies reported

(38) Peters, K. S.; Snyder, G. J. *Science* **1988**, *241*, 1053−1057.
(39) Hessler, D. P.; Frimmel, F. H.; Oliveros, E.; Braun, A. M. *J. Photochem. Photobiol. B:Biol.* **1996**, *36*, 55−60.
(40) Geiger, P. G.; Korytowski, W.; Lin, F. B.; Girotti, A. W. *Free Radical Biol. Med.* **1997**, *23*, 57−68.
(41) Anglin, J. H.; Batten, W. H. *Photochem. Photobiol.* **1970**, *11*, 271−277.

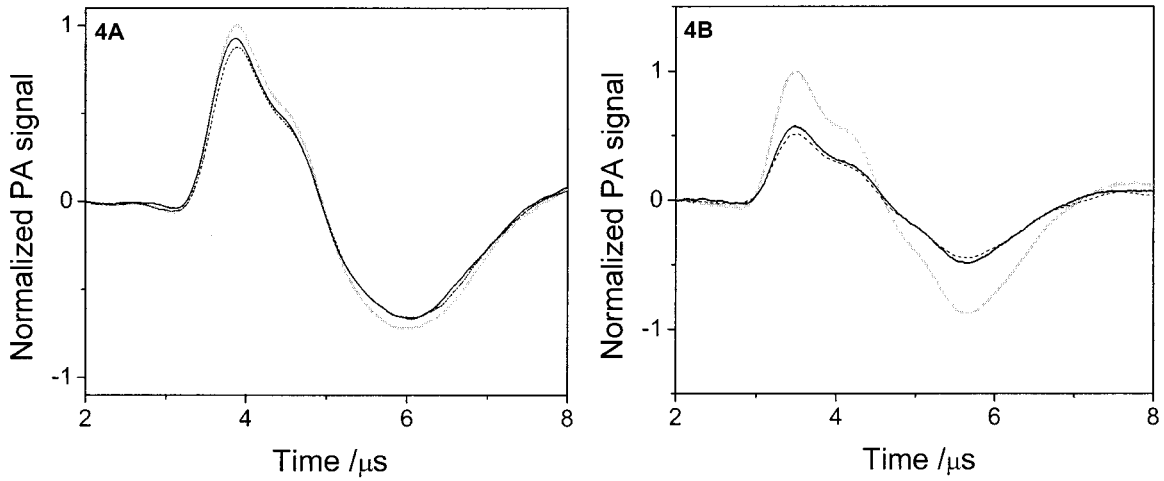

Figure 4. Normalized photoacoutic signal at 310 and 320 nm for BCP (solid gray) and *t*-UCA under oxygen (solid black) and *t*-UCA under argon (dashed). No shifts in the waveform between the reference BCP and *t*-UCA are observed. Figure 4A shows that at 310 nm the amplitude for the *t*-UCA signal is 90% of the BCP signal under argon. Figure 4B shows that at 320 nm the *t*-UCA signal has dropped to ~50% of the BCP signal under argon. There is more energy released under oxygen versus argon, which results in a 5% increase in the signal amplitude.

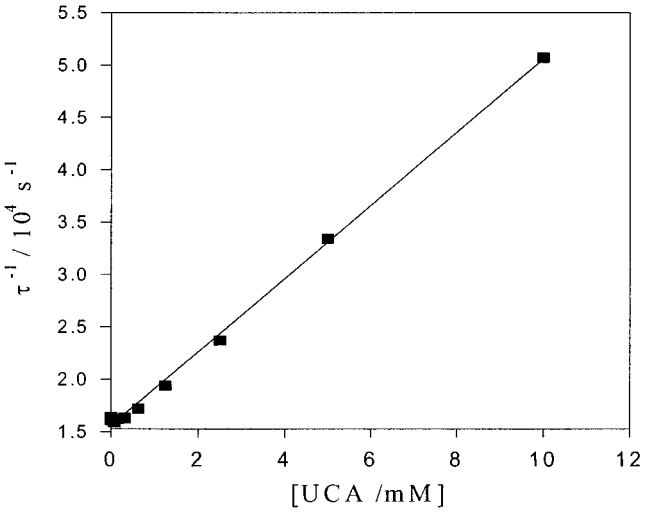

Figure 5. The reciprocal of the $^1O_2$ lifetime plotted against *t*-UCA concentration. The solid line is a linear fit to the data ($r^2 = 0.998$), which reveals a biomolecular quenching rate of $^1O_2$ by *t*-UCA of 3.5×10^6 M^{-1} s^{-1}.

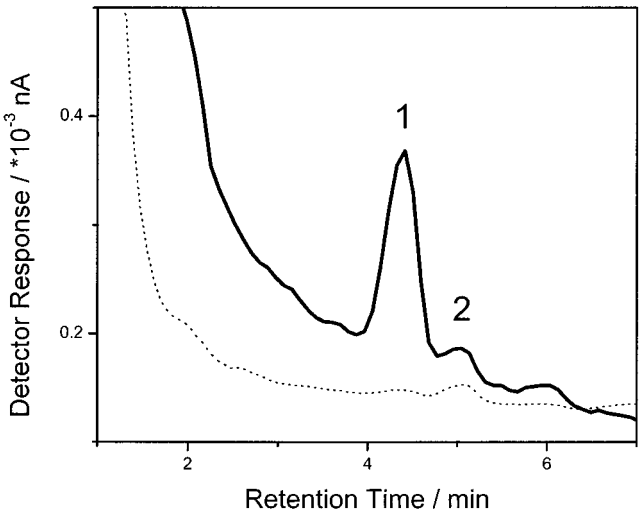

Figure 6. HPLC trace in 2-propanol showing the relative height of the peaks corresponding to 7α,β-ChOOH (peak 1) and 5α-ChOOH (peak 2) in the control (dotted line) and *t*-UCA (solid line) samples after 30 min irradiation.

herein, it is important to establish the spectroscopy is unaffected over the concentration range examined. The absorbance of *t*-UCA was examined as a function of concentration for the wavelength region 277 to 340 nm. This range covers not only the UV-A but spans the UV-B region, in which *t*-UCA exhibits wavelength-dependent isomerization yields. The UV-B region involves photoexcitation to different electronic states,[25] and the corresponding absorption features are sensitive to solvent and pH. If aggregation occurs between *t*-UCA molecules, spectral changes are anticipated. The data presented in Figure 2 establish the absorbance of *t*-UCA is linear with concentration over the entire range studied (0.01−10 mM). It is therefore reasonable to conclude the data reflect the photoreactivity of isolated *t*-UCA molecules in solution.

Morrison and co-workers reported the sum of the photoisomerization quantum yields at 313 nm for *c*-UCA and *t*-UCA is unity from which it was concluded isomerization is the only major photochemical event at this wavelength.[16] The data reported herein support this conclusion. The transient absorption data at 310 nm argue the initially prepared excited state decays with a time constant of ~1 ps. The decay of the transient absorption is complete and no residual bleach is observed, suggesting that the repopulation of the *t*-UCA ground state also occurs on this time scale. If isomerization is the only photochemical event at this excitation wavelength, the ground-state energy difference between the two UCA isomers can be calculated from the photoacoustic data at 310 nm.[25] Using the data in Table 1 for an excitation wavelength of 310 nm, $Q =$ 374 kJ mol^{-1} for *c*-UCA and $Q =$ 341 kJ mol^{-1} for *t*-UCA, resulting in a difference of 33 kJ mol^{-1} (at pH 7.3). Scaling by the quantum yield of isomerization at this wavelength (taken to be 0.5)[24] reveals the ground state of *t*-UCA lies 66 ± 15 kJ mol^{-1} below the ground state of the *c*-UCA isomer. Recent theoretical calculations by Page et al.[29] found the ground state to be 51.3 kJ mol^{-1} in favor of *t*-UCA, which is in good agreement with the above experimentally determined value.

It could be proposed that UCA isomerization is also the major photochemical process occurring for UV-A wavelengths longer than 313 nm, but quantum yields for UCA isomerization have not been determined for longer wavelengths. Recent studies

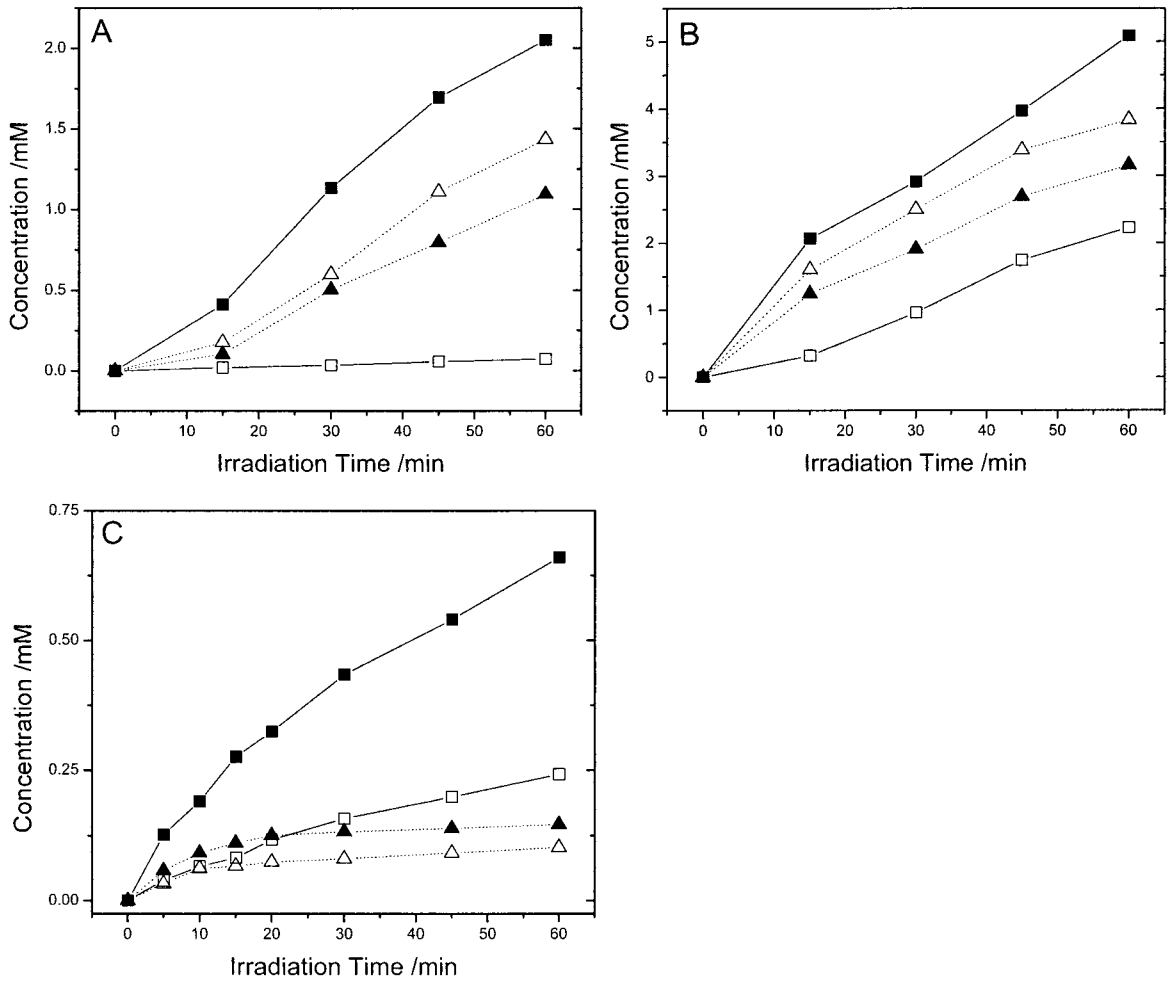

Figure 7. A plot of the HPLC analysis of the cholesterol hydroperoxidation assay showing the *t*-UCA sensitized photogeneration of 7α/*β*-ChOOH (squares, solid lines) and 5α-ChOOH (triangles, dashed lines) in the presence (solid symbol) and absence (open symbol) of *t*-UCA. Part A shows the results in the DMPC liposomes in H_2O. Part B shows the results in the DPMC liposomes in D_2O. Part C shows the results in 2-propanol.

establish that photoisomerization occurs following excitation of *t*-UCA in the UV-A (320 to 400 nm).[27] However as indicated in Table 1, the photoacoustic signal of *t*-UCA and *c*-UCA is strongly wavelength-dependent in the UV-A. For both isomers of UCA, there is a significant decrease in the percentage of the absorbed light released as heat with increasing wavelength. The small quantum yields for fluorescence (0.001−0.0001) and photodegradation (0.001) cannot account for this observation.[1] Hence, there must be additional photoreactive pathways for UCA which depend on the wavelength of UV-A light used.

Following excitation of UCA at pH 7.2, the possible initial photophysical processes include fluorescence, direct nonradiative relaxation to the ground state, isomerization, and intersystem crossing. The emission quantum yield is $\sim 10^{-4}$, and so this pathway is not important in the deactivation of the excited molecule. Because the isomerization time constant is on the order of a picosecond, direct nonradiative relaxation and isomerization result in nearly quantitative conversion of the absorbed energy into heat. Thus, the wavelength-dependent photoacoustic signals for *t*-UCA and *c*-UCA in the UV-A suggest intersystem crossing competes with these other processes in a wavelength-dependent manner. Consider then a model in which the excited state decays by competition between isomerization and intersystem crossing. The energy of the first excited triplet state, E_{triplet}, of *t*-UCA is ~230 kJ mol^{-1}.[16,25] Using this value and the above determined energy difference between the cis and trans isomer, E_{isomer}, an efficiency spectrum for triplet state formation can be calculated from the photoacoustic data as follows.[42] The total thermal energy Q released upon excitation is the sum of two contributions, indicated in eq 1. The first

$$Q = A_{\text{isc}}(E_{h\nu} - E_{\text{triplet}}) + B_{\text{iso}}(E_{h\nu} - \Phi E_{\text{isomer}}) \qquad (1)$$

term represents the heat released associated with intersystem crossing, assuming the triplet state lifetime is longer than the response of the photoacoustic detector.[25] The second term represents the heat release associated with isomerization. The coefficients A_{isc} and B_{iso} are the quantum yields for these two pathways, respectively, and Φ is the isomerization quantum yield over this wavelength range, taken to be 0.5 (the value at 313 nm).[24] Because there are only these two reaction pathways, $A_{\text{isc}} + B_{\text{iso}} = 1$, these coefficients can be determined from the photoacoustic and spectroscopic data.

Figure 8 shows the resulting efficiency spectra for triplet state formation for both isomers of UCA. Compared to *c*-UCA, *t*-UCA shows enhanced triplet production, but the two isomers show the same wavelength-dependent behavior. To determine an action spectrum for the photoproduction of triplet state

(42) Hanson, K. M.; Simon, J. D. *Proc. Natl. Acad. Sci. U S.A.* **1998**, *95*, 10576−10578.

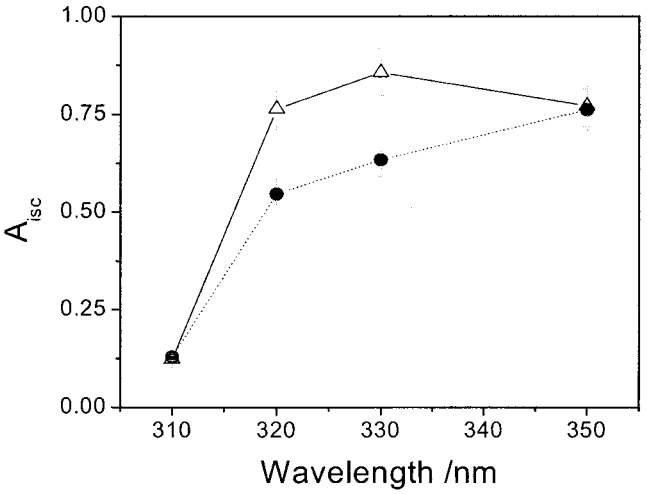

Figure 8. A plot of the calculated efficiency spectra for intersystem crossing, A_{isc}: *t*-UCA (triangles) and *c*-UCA (circles).

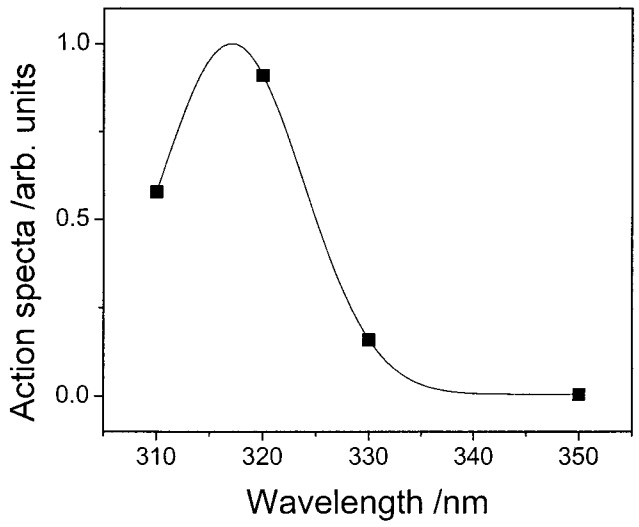

Figure 9. The normalized action spectrum for the formation of a long-lived triplet state of *t*-UCA at pH 7.3 with a Gaussian fit through the data resulting in a peak of ~320 nm.

molecules by *t*-UCA, the efficiency spectrum was scaled by the absorption coefficient of *t*-UCA at the wavelengths studied. The resulting action spectrum is shown in Figure 9. The shape of the action spectra is the same for *c*-UCA. The action spectrum peaks around 320 nm and is the same for aerobic and anaerobic samples.

As can be seen in Figure 4, oxygen versus argon saturated *t*-UCA solutions show a 5% to 10% increase in the amount of heat released. Previously reported the *t*-UCA triplet state can sensitize production of $^1O_2$,[42] and so this observed increase in photoacoustic signal under oxygen is attributed to $^1O_2$ production. Consider the data for 350 nm. Figure 8 shows a quantum efficiency for triplet production at this wavelength of ~0.8. If the quantum efficiency for $^1O_2$ production is 1.0, then we would expect a 50% increase in photoacoustic signal under oxygen compared to argon. The observed increase is significantly less, ~10%. These data can then be used to estimate the lifetime of the excited triplet state of *t*-UCA. While the photoacoustic data show the excited triplet state of *t*-UCA must persist onto the hundred(s) nanosecond time scale, the lifetime has never been measured directly. Attempts to observe the excited-state absorption with nanosecond flash photolysis have proved unsuccessful. The concentration of dissolved oxygen in aqueous solutions at 25 °C is ~0.26 mM[43] and the diffusion-controlled rate of quenching of excited triplets by oxygen is on the order of 10^9 s^{-1}.[44] The observed 10% increase in photoacoustic signal due to oxygen quenching of the *t*-UCA triplet establishes the lifetime of this excited state is on the order of 10^{-7} s^{-1}. The generation of excited triplet states of *t*-UCA upon UV-A exposure provides a mechanism for formation of reactive oxygen species (ROS). The efficiency and action spectra presented here indicate potential photochemical generation of ROS by UCA throughout the UV-A region.

Interestingly, the data in Figure 5 show *t*-UCA to also be an efficient scavenger of $^1O_2$. Morrison has previously reported *t*-UCA to be a good $^1O_2$ scavenger but kinetics were not discussed.[45] We find the bimolecular rate constant for $^1O_2$ scavenging by *t*-UCA to be 3.5×10^6 M^{-1} s^{-1}. *t*-UCA is not as good a scavenger as antioxidants such as β-carotene ($k_q = 1.4 \times 10^{10}$ M^{-1} s^{-1}),[46] but this rate constant is appreciable given the concentrations of *t*-UCA in the stratum corneum.

The photogeneration of ROS by *t*-UCA, and $^1O_2$ in particular, can be addressed from the cholesterol hydroperoxidation assay experiments. As indicated by the data in Figure 7, there is enhanced formation of 7α/β-ChOOH compared to the control with no *t*-UCA in all samples. This result implies UV-A excitation of *t*-UCA produces free radicals. Previous work by Morrison and Diebel shows that UV-A irradiation (>330 nm) of an electron affinic photosensitizing dye, nitro blue tetrazolium (NBT^{2+}), and *t*-UCA results in oxidation of *t*-UCA. These workers proposed this involved formation of a *t*-UCA radical.[47] In the presence of oxygen, irradiation of *t*-UCA and NBT^{2+} with light >275 nm, where the *t*-UCA absorption is competitive with NBT^{2+}, is also proposed to lead to the production of superoxide anion.[19] Production of superoxide anion or a *t*-UCA radical could account for the increased formation of 7α/β-ChOOH observed here.

Conversely, the 7α-ChOOH can also be formed by allylic rearrangement of the 5α-ChOOH species produced following $^1O_2$ attack. In D_2O, which should increase the $^1O_2$ lifetime, the rate of production of 7α/β-ChOOH increases, supporting such a mechanism. However, and more importantly, the rates of formation for 5α-ChOOH and 7α/β-ChOOH are comparable, which is not consistent with the conclusion 7α/β-ChOOH is formed solely by allylic rearrangement.

The data on the production of 5α-ChOOH with and without the presence of *t*-UCA at first appear perplexing. In the 2-propanol solvent, Figure 7C, the enhanced production of 5α-ChOOH in the presence of *t*-UCA relative to the control suggests there is production of $^1O_2$ by *t*-UCA. In D_2O, there is a further increase in production of 5α-ChOOH relative to H_2O, further supporting photochemical production of $^1O_2$. However, in the liposomal preparation as shown in Figure 7A,B, due to the inability to eliminate UV-A absorbing contaminants, there is always a background production of 5α-ChOOH in the control.

(43) Atkins, P. W. *Physical Chemistry*, 6th ed; Oxford University Press: New York, 1998.
(44) Bensasson, R. V.; Land, E. J.; Truscott, T. G. *Excited States and Free Radicals in Biology and Medicine*; Oxford University Press: Oxford, 1993.
(45) Morrison, H. *Photodermatology* **1985**, *2*, 158−165.
(46) Mascio, P. D.; Kaiser, S.; Sies, H. *Arch Biochem. Biophys.* **1989**, *274*, 532−538.
(47) Morrison, H.; Deibel, R. M. *Photochem. Photobiol.* **1986**, *43*, 663−665.

For the liposomal preparation, the amount of 5α-ChOOH produced decreases ~10% in the presence of *t*-UCA despite the fact that *t*-UCA generates $^1O_2$. This result can be explained by the fact *t*-UCA scavenges $^1O_2$. If one assumed *t*-UCA did not generate $^1O_2$, then using the rate of production of $^1O_2$ from the control and the scavenging rate of $^1O_2$ by *t*-UCA predicts there should be about half the 5α-ChOOH generated in the presence of *t*-UCA as in the control. Such a reduction in signal is not observed, further supporting the conclusion that *t*-UCA photogenerates $^1O_2$ upon UV-A excitation. The data observed in Figure 7A,B indicate *t*-UCA is a better scavenger than generator of $^1O_2$.

We now address the origin of the *t*-UCA wavelength-dependent efficiency for triplet state production in the UV-A. In a recent theoretical study of *t*-UCA, Page et al. confirm the initial excitation involves populating two overlapping electronic singlet states. The calculated vertical excitation energies for these states are in good agreement with experiment.[29] At 310 nm the lowest singlet state is populated, which gives rise to efficient isomerization. At 266 nm population of the second excited singlet state results in efficient intersystem crossing and little isomerization. For longer UV-A wavelengths, the data presented show competition between isomerization and intersystem crossing. In principle, there are many possible explanations for this behavior; including a weak direct excitation to a triplet state. While the exact mechanism is difficult to elucidate, recent gas-phase experiments on jet-cooled *t*-UCA offer insight into the observed wavelength-dependent behavior.

In their study of the gas-phase spectroscopy of *t*-UCA, Ryan and Levy identify three distinct energy regions of the excitation spectrum.[28] The lowest energy region is a collection of several well-resolved peaks and is proposed to be an excitation to the lowest singlet state. At slightly higher energy, there is an abrupt change where the peaks in the spectrum become broader and exhibit lower intensity. The highest energy region appears as an extremely broad feature, and is believed to represent excitation to a second excited singlet state.

Within the lowest energy region, the lines broaden with increasing energy. This reflects a shortening of the excited-state lifetime with increasing excitation energy. Broadening attributed to intramolecular vibrational redistributions occurs around 1000 cm^{-1} above the band origin. In Region II there is an alternation between sharp and broad spectra features but at 1600 cm^{-1} above the band origin, all features become broad. Excitation of these broad peaks produces dual emission attributed to radiative relaxation from *t*-UCA and *c*-UCA. Thus, the data support the conclusion there is an energy barrier to isomerization from the lowest singlet state.

On the basis of the gas-phase data, we propose there is also a barrier to the excited-state isomerization of *t*-UCA in solution. While the band origin in solution is difficult to determine, isomerization has been reported out to 340−400 nm.[27] Taking ~370 nm as a measure of the band origin, the time-resolved absorption data (Figure 3) were obtained exciting 3300 to 5300 cm^{-1} above the band origin. This is significantly higher than the magnitude of the reported isomerization barrier in the gas phase and it is reasonable to conclude molecules excited to this level travel ballistically over the potential energy barrier. If the nature of this electronic surface is similar to that of stilbene, passage over the barrier results in a twisted geometry, which upon relaxation to the ground electronic state finds itself at the top of the barrier between the cis and trans isomers. Nonradiative relaxation then generates nearly equal populations of the two isomers.[48] This could account for the ~0.5 quantum yield observed for *c*-UCA and *t*-UCA isomerization. At excitation energies below the barrier, the rate of isomerization is expected to be slower and other photophysical processes can compete.

We propose with decreasing excitation energy, intersystem crossing from the first excited singlet state competes more effectively with isomerization. On the basis of the data given in Table 1, excitation at 350 nm predominantly results in triplet state production. This suggests that excitation to 350 occurs in the vicinity near or below the barrier to isomerization in the first excited singlet state. This would place an estimate of the excited-state barrier at ~1500 cm^{-1} above the band origin, which is comparable to the gas-phase estimates. Unfortunately, the optical density of saturated *t*-UCA solutions for wavelengths greater than 330 nm is not sufficient for performing time-resolved measurements.

It is important to stress the weak absorption of *t*-UCA in the UV-A should not be overlooked because it not only results in isomerization but also in the generation of ROS and free radicals. While the quantum efficiencies of these latter processes must be quite small (≪1%), these reactive species may play a role in the UV-A induced biologic activity of *t*-UCA, including aging and carcinogenisis. Furthermore, the ability of *t*-UCA to scavenge ROS could be important in *t*-UCA's role in vivo.

Acknowledgment. This work is supported by the National Institute of General Medical Science and the Foundation for Polish Science (FNP-program Fastkin). We thank Dr Maurice Edington for his help in setting up the ultrafast pump−probe experiments performed on *t*-UCA.

JA016902X

(48) Todd, D. C.; Fleming, G. R. *J. Chem. Phys.* **1993**, *98*, 269−279.